ORIGINAL ARTICLE

Exploring Therapeutic Potentials of Natural Agents Against Breast Cancer Using Molecular Modeling

Moleküler Modelleme Kullanılarak Meme Kanserine Karşı Doğal Ajanların Terapötik Potansiyellerinin Araştırılması

[1]Nil Sazlı 🆔, [1]Deniz Karataş 🆔

[1] Manisa Celal Bayar University, Faculty of Engineering And Natural Sciences, Department of Bioengineering, Manisa, Türkiye

Correspondence

Deniz Karataş,
Manisa Celal Bayar University, Faculty of Engineering And Natural Sciences, Department of Bioengineering, Manisa, Türkiye

E-Mail: deniz.karatas@cbu.edu.tr

ABSTRACT

Background/Aims: This study examines the crystal receptor structure of the BRCA1 gene and its relationships with natural agents like curcumin, resveratrol, and quercetin, aiming to discover alternative natural agents to 5-Fluorouracil (5FU) and their therapeutic potential.
Method: The study focuses on the crystal structure of the BRCA1 gene, mutated into wild-type and mutant-type 3FA2, and evaluates binding affinities and structural stabilities with natural ligands like curcumin, quercetin, resveratrol, and 5FU chemical ligands.
Results: As a result of molecular dockings performed using mutant-type and wild-type 3FA2 receptors and natural agent and chemical drug ligands, the binding affinities of natural agents were found to be -6.6 kcal/mol and below, while the affinity score of the chemical drug ligand was -5.6 kcal/mol. RMSD, RMSF, Rg and RDF analyses performed as a result of molecular dynamics simulation show that receptor-ligand complex structures formed especially with natural agents have a very good stability. Among these structures, it was found that curcumin, which has the lowest binding score and stable values, has a strong binding affinity with receptors, a stable structure, and pharmacokinetic properties that carry the potential to be a good drug candidate compared to other ligands.
Conclusion: Curcumin, quercetin, and resveratrol indicate that natural agents may be alternative therapeutic drug candidates to the chemical drug 5FU in the treatment of breast cancer caused by BRCA1 gene mutation. Especially, curcumin has a good binding interaction score with receptors associated with BRCA1 genes, forms a stable structure, and has the expected pharmacokinetic profile, which promises hope for the discovery of new therapeutic natural agents for breast cancer treatment.

Keywords: Breast cancer, BRCA1, molecular docking, molecular dynamics simulation

ÖZ

Arka Plan/Amaçlar: Bu çalışma, BRCA1 geninin kristal reseptör yapısını ve kurkumin, resveratrol ve kuersetin gibi doğal ajanlarla ilişkilerini inceleyerek, 5-Florourasil (5FU)'e alternatif doğal ajanları ve bunların terapötik potansiyellerini keşfetmeyi amaçlamaktadır.
Yöntem: Çalışma, vahşi tip ve mutant tip 3FA2'ye mutasyona uğramış BRCA1 geninin kristal yapısına odaklanmakta ve kurkumin, kuersetin, resveratrol ve 5FU kimyasal ligandları gibi doğal ligandlarla bağlanma afinitelerini ve yapısal kararlılıklarını değerlendirmektedir.
Bulgular: Mutant-type ve wild-type 3FA2 reseptörleri ve doğal ajan ile kimyasal ilaç ligandları kullanılarak yapılan moleküler yerleştirmelerin sonucunda doğal ajanların bağlanma afiniteleri -6.6 kcal/mol ve altında değerlerde bulunurken kimyasal ilaç ligandının afinite skoru -5.6 kcal/mol değerindedir. Moleküler dinamik simülasyon sonucunda yapılan RMSD, RMSF, Rg ve RDF analizleri özellikle doğal ajanlar ile oluşturulan reseptör-ligand kompleks yapılarının oldukça iyi bir stabiliteye sahip olduğu sonucunu göstermektedir. Bu yapılardan en düşük bağlanma skoru ve stabil değerlere sahip kurkuminin diğer ligandlara kıyasla reseptörler ile güçlü bir bağlanma afinite, kararlı bir yapı ve iyi bir ilaç adayı olma potansiyelini taşıyan farmakokinetik özelliklere sahip olduğu bulgularına ulaşılmıştır.
Sonuç: BRCA1 gen mutasyonu kaynaklı meme kanseri tedavisinde kurkumin, kuersetin, resveratrol doğal ajanların kimyasal ilaç 5FU'ya alternatif ilaç adayları olabileceğini göstermektedir. Özellikle kurkuminin BRCA1 genleri ile ilişkili reseptörlerle iyi bir bağlanma etkileşim skoruna sahip olması, kararlı bir yapı oluşturması ve beklenen farmakokinetik profilinin olması meme kanseri tedavisine yönelik yeni terapötik doğal ajanların keşfedilmesi için umut vaadetmektedir.

Anahtar Kelimeler: BRCA1, meme kanseri, moleküler yerleştirme, moleküler dinamik simülasyon

Introduction

The most well-known type of cancer, whose incidence is increasing day by day worldwide, is breast cancer. It is characterized by normal cells in the breast area becoming abnormal and multiplying uncontrollably, leading to the formation of malignant tumor cells (1, 2). Given that this type of cancer has led to a rise in the mortality rate among women in recent years, it has become an even more serious disease for which alternative treatment methods must be sought (1).

One of the major factors contributing to the onset of breast cancer is mutations in genes (3, 4). The most well-known gene associated with breast cancer is BRCA1 (Breast Cancer Gene 1). The BRCA1 gene is a tumor suppressor gene that regulates cell division and the repair of DNA damage (5). This tumor suppressor gene encodes a protein that plays a role in repairing damaged DNA mechanisms, thereby preventing abnormal cell division and the formation of breast

cancer by restoring the damaged DNA mechanism (6, 7). As a result of the mutation of the BRCA1 gene, the DNA repair mechanism does not function properly, leading to negative events such as DNA damage, unrepaired DNA, and abnormal cell growth and division (5, 6). The occurrence of these conditions caused by mutations in the BRCA1 gene increases the risk of developing breast cancer and accelerates the progression of existing cancer (8). For all these reasons, the BRCA1 gene, a tumor suppressor gene, is crucial for maintaining genomic stability, and mutations in this gene pose significant challenges in the treatment of breast cancer. (9). For this reason, it is crucial to explore alternative treatment methods, especially for breast cancer caused by BRCA1 gene mutations (10, 11).

When literature studies are examined, methods such as radiotherapy, chemotherapy, and immunotherapy are utilized in the treatment of various types of cancer, particularly breast cancer (12). Radiotherapy slows down the growth of cancerous cells and destroys them with the assistance of high-energy rays. The high-energy rays utilized in this method fragment the DNA material within cancer cells (5). In this way, it leads to the death of cancerous cells. Radiotherapy, also known as radiation therapy, aims to eliminate potentially cancerous cells left behind after lumpectomy and mastectomy in BRCA1-related breast cancer type (12, 13). In chemotherapy, drugs targeting cancer cells are utilized to eliminate damaged cells. This method is employed to reduce tumor size before surgical procedures or to eradicate cells deemed potentially cancerous post-surgery. Immunotherapy is a significant method capable of enhancing DNA repair mechanisms and anti-tumor immune responses (14, 15). These methods are the most common treatment options utilized in addressing various types of cancer such as breast cancer. However, while these treatments combat cancer, they also induce numerous side effects on the human body (16, 17). For example, following radiotherapy, patients may experience fatigue, hair loss, difficulty breathing and swallowing; increased risk of infection and anemia may occur after chemotherapy; susceptibility to autoimmune diseases after immunotherapy can lead to irregularities in the functions of vital organs such as the liver (18). For these reasons, it is important to discover alternative solutions in the treatment of breast cancer caused by BRCA1 gene mutations that do not have side effects on human health (19).

It is crucial to utilize therapeutic natural agents in the treatment of breast cancer that have minimal side effects on human health. Naturally sourced agents such as plant extracts and algae pigments exhibit anticancer properties by combating cancerous cells (20). Thus, it is of great importance for human health to discover new treatment methods using alternative therapeutic drug agents instead of treatment practices that involve chemical drugs and their associated side effects (17). The natural agents curcumin, resveratrol, and quercetin obtained from extracts of turmeric, red grapes, and various fruits and vegetables used in this study possess numerous bioactive properties (20, 21). Curcumin exhibits antioxidant properties by combating free radicals and oxidative stress in the body. Additionally, it possesses anti-inflammatory properties for conditions such as inflammation in the body, and it has anti-cancer properties by fighting cancer cells (21). Resveratrol battles free radicals similar to curcumin. It safeguards the DNA mechanism from oxidative damage through its antioxidant properties. Additionally, it combats cancerous cells by inhibiting the proliferation of breast cancer cells (22, 23). Another natural agent, quercetin, is a flavonoid. It possesses bioactive properties such as antioxidant and anti-inflammatory effects. This natural agent prevents the growth of cancerous cells by stimulating apoptotic processes (24). In this way, it addresses situations such as metastasis, causing tumor cells to spread to other parts of the body (25).

In the literature studies of Thai et al., it was emphasized that BRCA1 somatic gene mutations are associated with breast cancer (26). In addition, many literature studies have revealed that the valine amino acid at position 695 in the BRCA1 gene is mutated and somatically transformed into a leucine amino acid, and its relationship with breast cancer (26, 27). The utilization of molecular modeling approaches with different perspectives, such as molecular docking and molecular dynamics simulation, in studies found in the literature, will shed light on the discovery of treatment methods for vital diseases such as breast cancer (28, 29). Taking the studies of Thai et al. as a reference, within the scope of this study, the valine amino acid at position 695 of the A chain bound by the ligand was mutated by converting it to leucine in the crystal structure receptor with double chain 3FA2 PDB ID, A and B, obtained from the Protein Data Bank (PDB) (26). It was aimed to discover a new treatment method by performing molecular docking and molecular dynamics simulations of the obtained

mutant-type 3FA2 and wild-type 3FA2 receptors with the chemical drug 5-Fluorouracil (5FU), as well as such natural agents as curcumin, resveratrol, and quercetin ligands, which are among the most widely used drugs in the treatment of breast cancer in the market. One of the main aims of this study on breast cancer caused by BRCA1 gene mutation is to understand the interaction of ligands selected as therapeutic natural agents in breast cancer treatment with wild-type and mutant-type receptors associated with the BRCA1 gene, and to compare the biological structure of the mutant-type complex with the wild-type structure, giving meaning to their functions.

Within the scope of this study, the relationship between the wild-type and mutant-type 3FA2 crystal receptor structures, obtained by normal and point mutation of the BRCA1 gene associated with breast cancer, and chemical drug and natural agent ligands was examined through molecular docking. The mutation mechanism was analyzed by examining the molecular docking results in both wild-type and mutant-type receptor structures. A molecular dynamics simulation was conducted based on the docking results obtained. As a result of the simulation, graphics including RMSD (Root Mean Square Deviation), RMSF (Root Mean Square Fluctuation), Rg (Gyration Radius), and RDF (Radial Distribution Function) were obtained. Due to the data obtained, the therapeutic potential of the natural agents curcumin, resveratrol, and quercetin, as well as the chemical agent 5FU, on the wild-type and mutant-type receptors associated with the BRCA1 gene, was analyzed. The pharmacokinetic and pharmacodynamic properties of the ligands belonging to the most stable and favored conformations obtained as a result of docking and MD simulations were compared with ADMET analysis, revealing that these ligands possess therapeutic bioactive components. In summary, this literature study aimed to demonstrate that natural agents such as curcumin, resveratrol, and quercetin serve as new drug agents of natural origin, showcasing their therapeutic potential in breast cancer caused by gene mutations to be as effective as chemical drugs. This research contributes to the exploration of alternative treatment methods for breast cancer caused by BRCA1 gene mutation.

Computational Setup

Provision and Mutation of The Receptor

Criteria such as resolution, organism, and PDB validation table values of many receptor structures related to

the BRCA1 gene were analyzed for use in this study. The Crystal Structure of the BRCA1 Associated Ring Domain (BARD1) Tandem BRCT Domains structure with PDB ID 3FA2, which has two repeated chains, A/B, and a resolution of 2.20 Å, was chosen as the most suitable structure. The 3FA2 receptor Figure 1 was obtained in 3D format from the Protein Data Bank (https://www.rcsb.org/) (30).
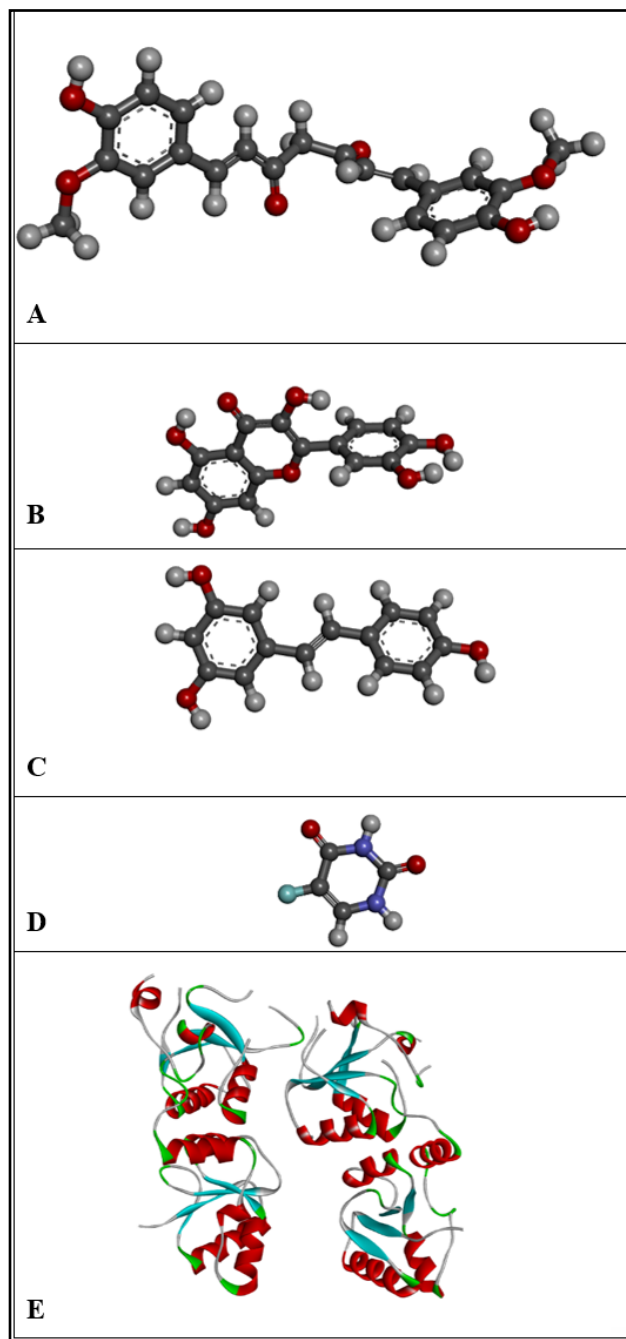
Figure 1. The structures of the ligand molecules shown in 3D models. The ligands are the chemical drug substance curcumin (A), quercetin (B), resveratrol (C), and 5FU (D). Dark gray, light gray, red, blue, and cyan colors for ligands are carbon (C), oxygen (H), oxygen (O), nitrogen (N), and fluorine (F), respectively. Red and blue ribbons for the 6M14

structure are A and B chains, respectively. The receptor is the solution Crystal Structure of the BRCA1 Associated Ring Domain (BARD1) Tandem BRCT Domains (PDB code: 3FA2) (E). The 3FA2 structure comprises two chains, designated as A and B, respectively.

The 3FA2 crystal receptor structure was opened using the PyMOL program. Later, based on the location of the breast cancer mutation associated with the BRCA1 gene in their study, Thai et al. transformed the VAL amino acid at position 695 in the A chain into the LEU amino acid, and somatic mutation was carried out (26, 27). Since the ligand-binding region of the 3FA2 receptor is on the A chain, it was decided that the mutation would only occur in the A region of this structure, which has A and B chains. At the end of all these stages, in this study, both mutant-type and wild-type 3FA2 receptors were obtained to understand the interactions between mutated and unmutated receptors, natural agents, and chemical drugs (27, 31).

Preparation of Receptors for The Docking Step

3FA2 receptors, both wild-type and mutant-type, were opened separately using USCF Chimera 1.17.3. Template ligands, such as GOL and PO4, along with water molecules, were deleted from the receptor structures. The structures underwent the dock prep process and were saved in '.mol2' format. Both receptor structures, wild-type, and mutant-type 3FA2, were then prepared for the molecular docking step (30, 32).

Preparation of Ligands for The Docking Step

Within the scope of this study, one drug and three natural agents, 5FU, curcumin, resveratrol, and quercetin, were selected as ligands. These ligand structures were obtained in 3D format from PubChem (https://pubchem.ncbi.nlm.nih.gov/). Each ligand structure was opened via USCF Chimera 1.17.3. Hydrogens were added to minimize the ligands, and the charge assignment process was applied. Then, the charges of the ligands were neutralized and recorded in '.mol2' format. The ligands are now ready for the docking phase.

Determination of The Active Regions of The Receptors

The position of the binding site amino acids, created with the template ligands of the crystal structure with PDB ID 3FA2, was examined in the PDB. It was determined that the binding site of the 3FA2 receptor is around amino acids at positions 650 to 750. In line

with this information, the AutoGridFR 1.2 program, a bioinformatics tool, was used to determine the coordinates of the active site (33). The 3FA2 receptor and ligands, converted to the '.pdbqt' format via the AutoDock Vina program, were transferred to the AutoGridFR 1.2 program. Binding site amino acids at positions 650 to 750, referenced from the PDB, were selected. A target file with a '.trg' extension was created. The codes required to create a grid box were written in the Git CMD interface (27, 33). These steps were also repeated for the mutant-type 3FA2. According to the coordinates obtained, grid box parameters were determined for the docking stages with wild-type and mutant-type receptors and various ligands. In wild-type and mutant-type 3FA2 structures, the grid box parameters are 11.451, 18.284, and -35.160 for the center and 70, 70, and 70 for size, respectively, according to the XYZ coordinates.

Molecular Docking Analysis

A previously prepared receptor and a ligand in '.mol2' format were opened one above the other in the USCF Chimera 1.17.3 program. Using the Surface/Binding Analysis and AutoDock Vina options in the program, the previously determined grid box parameters were set for the appropriate receptor and ligand. Then, docking was performed (34, 35). In this step, eight docking processes were performed by applying wild-type and mutant-type 3FA2 receptors and 5FU, curcumin, resveratrol, and quercetin ligands. As a result of the docking processes for all receptor-ligand pairs, eight different lowest binding energy scores were obtained.

Molecular Dynamics Simulation

A 25 ns molecular dynamics simulation was performed via the GROMACS program to understand the stability, energy interactions, and hydrogen bond analysis of the receptor-ligand complex structures obtained from the eight lowest binding energy scores for each receptor and ligand (34). As a result of the simulation, RMSD (Root Mean Square Deviation), RMSF (Root Mean Square Fluctuation), gyration radius, and RDF (Radial Distribution Function) graphs were drawn to understand the interaction between receptors and ligands. The obtained results were analyzed and interpreted (4, 10).

Results

Molecular Docking and Interaction Analysis

A separate docking process is carried out with the

natural agents, including curcumin, quercetin, and resveratrol, which are predicted to have therapeutic potential in the treatment of breast cancer associated with mutant-type and wild-type 3FA2 receptors and the BRCA1 gene, as well as with the chemical drug 5FU, which is widely used in the market. The result of these receptor-ligand complexes is the binding affinity data shown in Table 1.

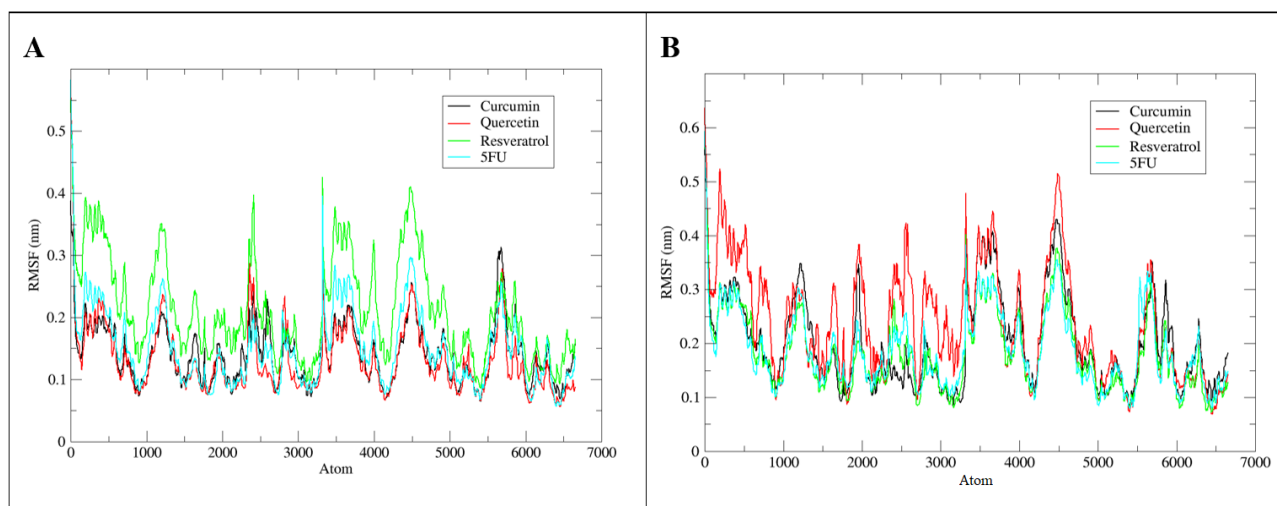**Table 1.** Energy-based docking results for each model.

Receptor	Name of Ligand	Binding affinity (kcal/mol)
Mutant-type 3FA2	Curcumin	-7.8
	Quercetin	-7.9
	Resveratrol	-6.6
	5FU	-5.8
Wild-type 3FA2	Curcumin	-7.6
	Quercetin	-8.1
	Resveratrol	-6.8
	5FU	-5.6

Binding affinities obtained with curcumin, quercetin, resveratrol, and 5FU for the mutant-type 3FA2 receptor, which was created by somatic mutation by converting the VAL amino acid at position 695 in the A chain to the LEU amino acid of the crystal structure with PDB ID 3FA2 associated with the BRCA1 gene, are -7.8, -7.9, -6.6, and -5.8 kcal/mol. The results obtained from the docking phase of the wild-type 3FA2 receptor and the ligands are -7.6, -8.1, -6.8, and -5.6 kcal/mol.

The interactions of complexes formed between mutant-type 3FA2 and wild-type 3FA2 receptors, along with other ligands, are depicted in Figure 2 and Figure 3, respectively. The Discovery Studio 2021 Client program was employed to visualize the interactions within the receptor and ligand complex. In A1 of Figure 3, the bond interactions between the 3FA2 receptor and the curcumin ligand resulting from docking are observed. Curcumin interacts with the receptor through the Van der Waals amino acid Serine (SER) at position 761. Additionally, amino acids Serine (SER), Lysine (LYS), and serine (SER) numbered 616, 688, and 760, respectively, are also visible. Additionally, alkyl and pi-alkyl interactions are evident in amino acids 680, 684, and 764, namely Lysine (LYS), Isoleucine (ILE), and Tryptophan (TRP). Amide-pi stacked interactions are also evident in the receptor-ligand complex map obtained after A2 docking in Figure 3. When examining the receptor-ligand map of the wild-type

3FA2 and quercetin receptor in A2 after docking, conventional hydrogen bonds are observed at amino acid residues Arginine (ARG) and Tyrosine (TYR) at positions 705, 745, and 678, respectively. Additionally, unfavorable donor-donor interactions are observed between amino acid number 765 of asparagine (ASP) and amino acid number 688 of Lysine (LYS). Upon examination of the wild-type 3FA2 and resveratrol complex map in A3, a pi-donor hydrogen bond is found in the SER amino acid at position 616, van der Waals interaction in the SER amino acid at position 761, and a conventional hydrogen bond in the 686th Histidine (HIS) amino acid, 688th LYS. Additionally, there is pi-cation interaction, amide-pi stacking at SER at position 760, and pi-alkyl interactions at the ILE amino acid at position 764. In the A4 image in Figure 2, in the complex formed with the 5FU ligand and mutant-type 3FA2, conventional hydrogen bonds are present in the HIS and GLU amino acids at positions 686 and 740. Carbon hydrogen bonds and pi-donor hydrogen bonds are present in the HIS amino acid at position 685 and the SER amino acids at positions 760 and 761. When examining the interaction of the 5FU ligand and wild-type 3FA2 complex with amino acids in the A4 image in Figure 3, there are conventional hydrogen bonds and unfavorable hydrogen bond interactions in the HIS amino acid at position 686. While there is only a conventional hydrogen bond in the GLU amino acid at position 740, there are pi-donor hydrogen bonds in the SER amino acids at positions 760 and 761. Upon inspecting the curcumin complex map in B1 of Figure 3 after MDS, it is observed that amino acids PRO, ALA, Glutamic acid (GLU), and Methionine (MET) are located at positions 610, 613, 655, and 768, respectively. When examining the receptor-ligand maps of the mutant-type 3FA2 and various ligands after docking and MDS in images A1 and B1 in Figure 2, it is observed that the amino acids TRP at position 680, LYS at position 688, SER at position 761, ASP at position 765, and MET at position 768 remain consistent. When images A2 and B2 in Figure 3 are examined, it is observed that the amino acids ARG, ASP, and LEU, numbered 705, 763, and 773, respectively, remain unchanged in the quercetin complex map. Additionally, In the B4 image in Figure 2, in the complex formed with the 5FU ligand and mutant-type 3FA2, the amino acids GLY at position 681 and SER at position 761 contain carbon-hydrogen bonds, THR at position 682 and GLU at position 740 contain conventional hydrogen bonds, ASP at position 741 contains unfavorable donor-donor interactions, and HIS at position 685 contains

pi-pi stacked interactions. In the B4 image in Figure 3, when examining the interaction of the 5FU ligand and wild-type 3FA2 complex with amino acids, LYS at position 684, GLU at position 740, and SER at position 760 contain conventional hydrogen bonds, and HIS at position 685 contains unfavorable donor-donor and pi-pi stacking interactions.

Root Mean Square Fluctuation (RMSF)

RMSF values for receptor-ligand complexes, comprising four distinct ligands - namely, curcumin, quercetin, resveratrol, and 5FU - utilizing the mutant-type 3FA2 receptor depicted in Figure 4A, are presented. Throughout the 25 ns simulation, the mean RMSF values of the complex structures involving the mutant-

Figure 2. The images generated by Discovery Studio 2021 Client depict interactions between the ligands curcumin, quercetin, resveratrol, 5FU, and the mutant-type 3FA2 receptor, respectively. The top row modes represent the lowest binding conformations calculated in binding studies **(A1, A2, A3, A4)**, while the bottom row frames represent final snapshots from MD simulations **(B1, B2, B3, B4)**, respectively.

Figure 3. The images generated by Discovery Studio 2021 Client depict interactions between the ligands curcumin, quercetin, resveratrol, 5FU, and the wild-type 3FA2 receptor, respectively. The top row modes represent the lowest binding conformations calculated in binding studies **(A1, A2, A3, A4)**, while the bottom row frames represent final snapshots from MD simulations **(B1, B2, B3, B4)**, respectively.

Figure 4. RMSF graph depicting the fluctuations of the mutant-type 3FA2 receptor **(A)** and wild-type 3FA2 receptor **(B)** in complex with ligands, respectively.

type 3FA2 receptor paired with curcumin, quercetin, resveratrol, and 5FU ligands are 0.20, 0.15, 0.30, and 0.25 nm, respectively. Upon detailed examination of the RMSF graph of the mutant-type 3FA2 and curcumin complex, peaks are observed at atoms 2347, 3472, and 4521. Similarly, in the RMSF graph of the complex formed with quercetin, peaks are identified at atoms 2353, 3337, 4508, and 5692. In the RMSF graph of the mutant-type 3FA2 and resveratrol complexes, peak values are observed at atoms 1182, 2424, 3305, and 4476. Additionally, in the RMSF graph of the complex formed with 5FU, peak values occur at atoms 1203, 3333, 4490, and 5567. Figure 4B depicts the RMSF graphs of the receptor-ligand complexes formed with the wild-type 3FA2 receptor and four different ligands:

curcumin, quercetin, resveratrol, and 5FU. The average RMSF values of the complex structures formed with curcumin, quercetin, resveratrol, and 5FU ligands of the wild-type 3FA2 receptor are 0.20, 0.30, 0.25, and 0.28 nm, respectively. Upon examination of the RMSF graph of the wild-type 3FA2 and curcumin complex, peaks are observed at atoms 1206, 1937, 3656, and 4464. In the RMSF graph of the complex formed with quercetin, peaks are identified at atoms 3310 and 4471. Furthermore, in the RMSF graph of wild-type 3FA2 and resveratrol complexes, it is noted that the values peak at atomic positions similar to quercetin.

Radial Distribution Function (RDF)

The RDF graphs of the complexes formed by curcumin,
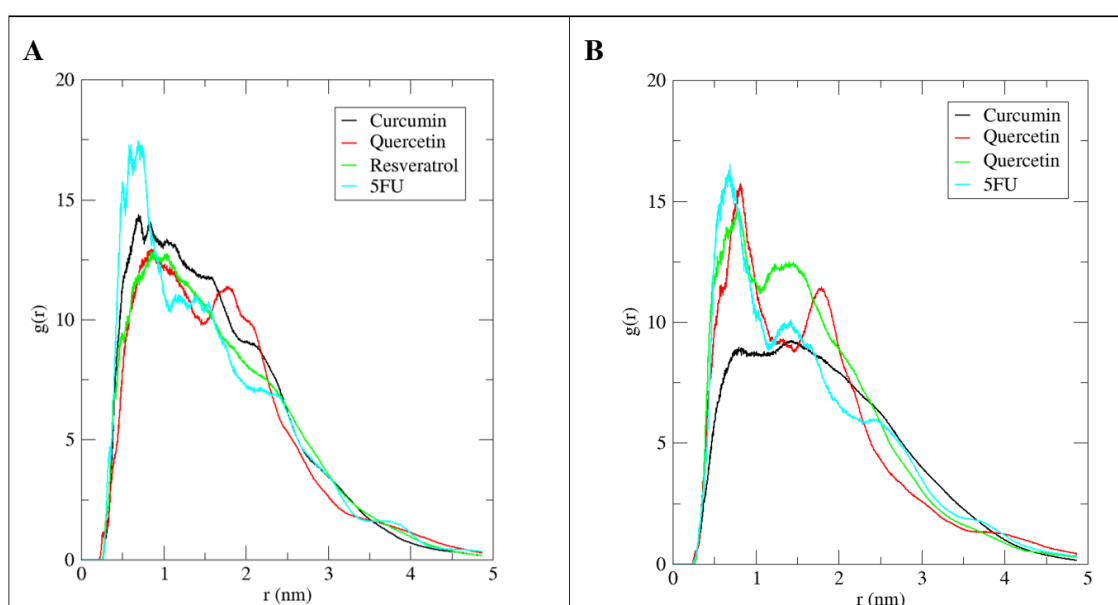
Figure 5. RDF graph illustrating the radial distribution function between the ligands and the binding sites of the mutant-type 3FA2 receptor **(A)** and wild-type 3FA2 receptor **(B)**, respectively.

quercetin, resveratrol, and 5FU ligands with the mutant-type and wild-type 3FA2 receptors during the 25-nanosecond molecular dynamics simulation are shown in Figure 5. Upon inspection of the values for the complex formed with curcumin in Figure 5A, a peak is observed at 0.81 nm with a value of 13.23. The peak value for the quercetin complex is 12.91 at 0.84 nm. Although a distinct peak is not observed in the resveratrol complex, its highest value is 17.75 at 0.86 nm. 5FU is at a distance of 17.48 with a value of 0.73 nm. The graphical results show that curcumin and quercetin ligands are densely present in the receptor structure at a distance of 1 nm and establish strong interactions. When examining the RDF graphs depicted in Figure 5B, it is observed that the complex formed with the natural agent curcumin and the wild-type 3FA2 receptor lacks a distinct peak point. However, the highest value is 9.23 at a distance of 1.40 nm. In contrast, distinct peak points are observed in the RDF values for the complexes formed with quercetin and resveratrol. These values are 15.46 at 0.81 nm and 14.64 at 0.77 nm, respectively. There is a distinct peak in the chemical ligand 5FU complex. If it is necessary to specify the peak value of the RDF value, it is 16.34 at 0.67 nm.

Root Mean Square Deviation (RMSD)

The results of the RMSD analyses conducted to examine the stability of the protein and ligand complexes are shown in Figure 6. When examining the RMSD values of different ligand complexes with the mutant-type 3FA2 receptor in Figure 6A, it is evident that the graphs of the curcumin and quercetin complexes exhibit remarkable stability. The values for these two

complexes range from 0.2 to 0.3 nm. The resveratrol complex was observed to stabilize at approximately 0.2 nm after 6.80 ns. The graph of the 5FU complex progresses quite stable throughout the simulation. The average RMSD values of this complex are around 0.3 nm. In the RMSD graphs of the wild-type 3FA2 receptor and various ligand complexes in Figure 6B, the curcumin complex exhibits overall stability. Upon closer inspection, it adopts a more stable form around 1.43 nm after 13 ns. Similar results were obtained for the graphs of the quercetin and resveratrol complexes. The RMSD values of both complexes are around 0.5 nm, indicating a highly stable graph representation. The graph of the receptor-ligand complex formed with 5FU, a chemical ligand, is quite stable. In general, stability was reached around 0.4 nm after 3 ns of simulation.

Radius of Gyration (Rg)

Rg analyses were conducted to understand the compactness of the complexes formed by the mutant-type and wild-type 3FA2 receptors with curcumin, quercetin, resveratrol, and 5FU ligands. The Rg analysis data for all structures are shown in Figure 7. When examining the Rg graphs of the mutant-type 3FA2 receptor and other ligand complexes in Figure 7A, it is observed that the values of the curcumin complex remained stable at around 2.5 nm throughout the 25 ns simulation period, corresponding to 25000 ps. The quercetin complex exhibited stability around 2.3 nm between 5 and 16 ns, although some fluctuations are present in the graph. The Rg values obtained for the resveratrol complex fluctuated between 2 and 2.5 nm. 5FU showed values around 2.48 nm. When the
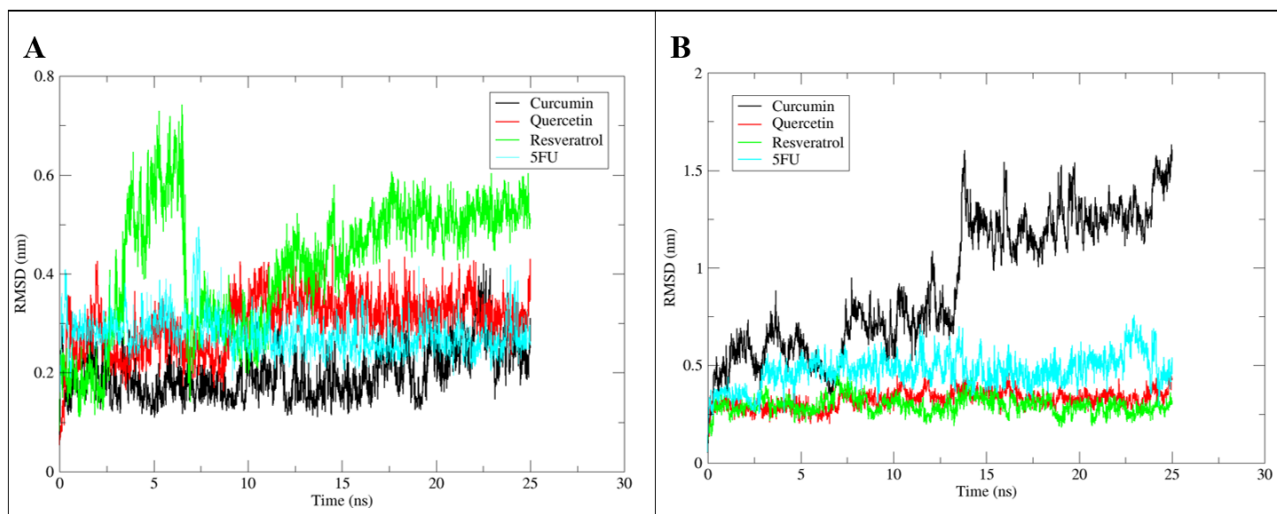
Figure 6. RMSD graph showing the structural deviations of the mutant-type 3FA2 receptor **(A)** and wild-type 3FA2 receptor **(B)** during the simulation in the presence of ligands, respectively.
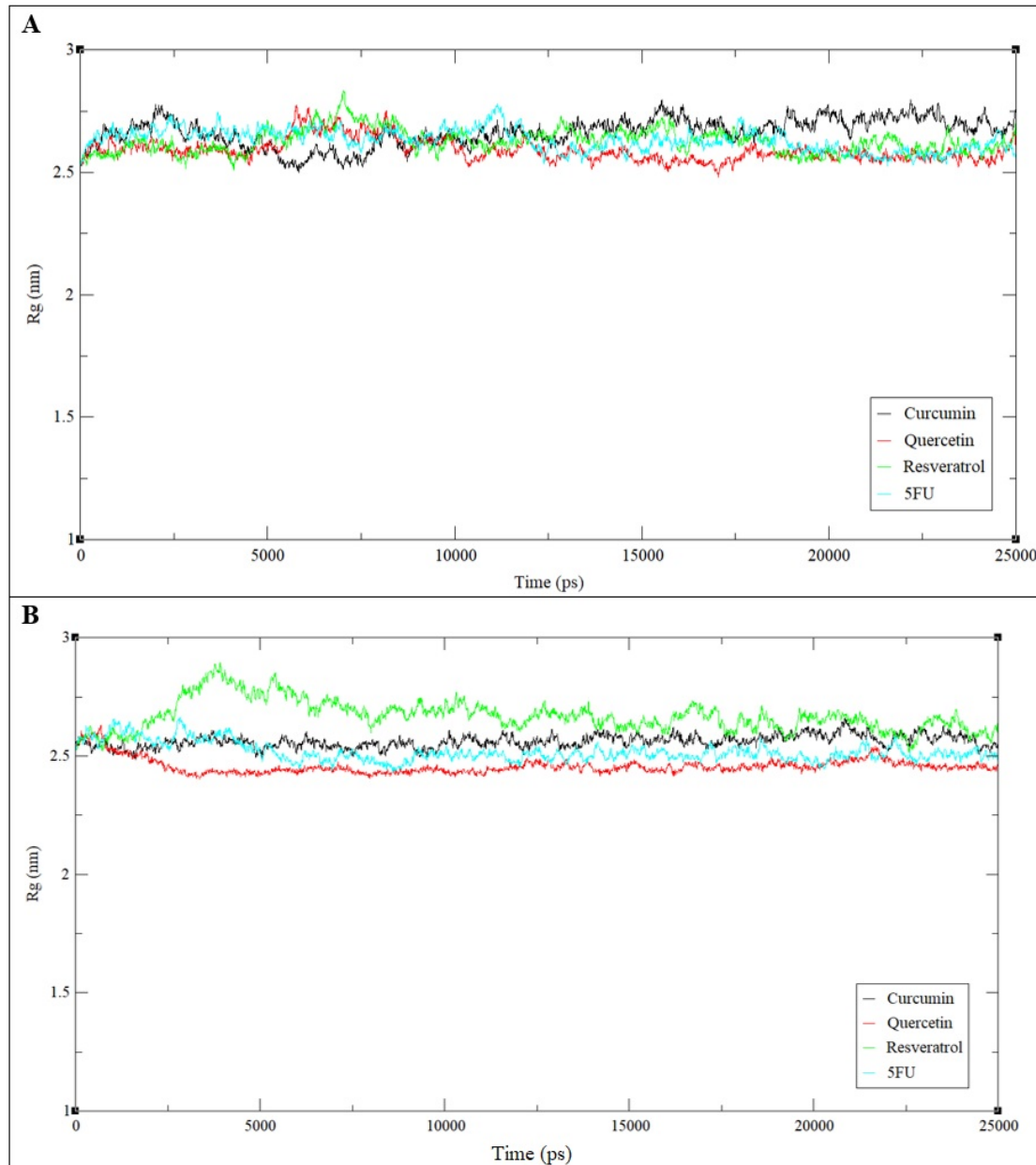
Figure 7. Rg graph representing the compactness of the mutant-type 3FA2 receptor **(A)** and wild-type 3FA2 receptor **(B)** in complex with ligands throughout the simulation, respectively.

Rg graphs of the wild-type 3FA2 and different ligand complexes in Figure 7B are examined, it is observed that the Rg values of the complex formed with curcumin ranged between 2.4 and 2.6 nm throughout the simulation. The quercetin complex fluctuated between 1.75 and generally 2 nm, the resveratrol complex ranged generally between 2.18 and 2.4 nm, and finally, the 5FU complex hovered around 2.5 nm. The value of the complex formed with curcumin is higher than the other ligands, but the difference is only 0.1 nm. The quercetin complex stabilized around 2.3 nm after 7.5 ns. In the resveratrol complex, a smoother graph is observed around 1 ns at approximately 2.5 nm, yet increasing fluctuations persist throughout

the simulation period. The average Rg values of the 5FU ligand complex throughout the simulation are between 2.4 and 2.6 nm, but there is a constant fluctuation.

ADMET Properties Prediction of Ligand Molecules

When examining the data in Table 2, the results of ADMET analysis of the complexes formed by the mutant-type 3FA2 receptor with different natural agent ligands after docking and MDS are observed. In the docking results section, curcumin exhibits a Consensus Log Po/w value of 3.03, indicating its high lipophilic properties. While the Log Kp (skin permeation) value was -6.28 cm/s in the data obtained after docking, it

decreased to -2.28 cm/s post-MDS. When examining Table 3 for the ADMET analyses of wild-type 3FA2 and natural ligands after docking and MDS, similar results to Table 2 are observed. In Table 3, while the Consensus Log P/o (Log Po/w) value of the quercetin ligand after docking was 1.23, it decreased to 0.51 after MDS. The ADMET analysis results generally demonstrate favorable outcomes for each natural agent for both the mutant-type and wild-type 3FA2 receptors. Based on these analyses, curcumin emerges as the ligand with the most favorable properties. Subsequent data for both docking and MDS of ADMET assays obtained with mutant-type and wild-type 3FA2 receptors of the 5FU ligand in Table 2 and Table 3 are identical. This ligand is generally good as a drug.

Discussion

Within the scope of this study, natural and chemical ligands of mutant-type and wild-type 3FA2 receptors associated with the BRCA1 gene were analyzed using molecular modeling techniques such as molecular docking and molecular dynamics simulations. As a result of these analyses, the binding affinities and structural stability of the receptor-ligand complex structures were evaluated. According to the findings, it is an expected result that 5FU, which is widely used in the treatment of breast cancer, has a high affinity with the receptors. The fact that the docking results obtained with natural agents are higher than -6 kcal/mol, and especially the result of the quercetin ligand being even better than the 5FU ligand, shows that natural agents provide a

Table 2. ADMET properties prediction results for ligands from mutant-type.

Results	Ligand	Con-sensus Log Po/w	Log Kp (skin) perme-ation, cm/s	GI Absorp-tion	BBB Perme-ant	P-gp Subst-rate	CY-P1A2 Inhibi-tor	CY-P2C19 Inhibi-tor	CY-P2C9 Inhibi-tor	CY-P2D6 Inhibi-tor	CY-P3A4 Inhibi-tor	Bioa-vaila-bility Score
Docking	Curcumin	3.03	-6.28	High	No	No	No	No	Yes	No	Yes	0.55
	Quercetin	1.23	-7.05	High	No	No	Yes	No	No	Yes	Yes	0.55
	Resveratrol	2.48	-5.47	High	Yes	No	Yes	No	Yes	No	Yes	0.55
	5FU	0.13	-7.73	High	No	No	No	No	No	No	No	0.55
MD	Curcumin	3.03	-2.28	High	No	No	No	No	Yes	No	Yes	0.55
	Quercetin	1.23	-7.05	High	No	No	Yes	No	No	Yes	Yes	0.55
	Resveratrol	2.49	-5.52	High	Yes	No	Yes	No	No	Yes	Yes	0.55
	5FU	0.13	-7.73	High	No	No	No	No	No	No	No	0.55

Table 3. Wild-type 3FA2 receptors and natural agents ligands ADMET properties prediction results.

Results	Ligand	Con-sensus Log Po/w	Log Kp (skin) perme-ation, cm/s	GI Absorp-tion	BBB Perme-ant	P-gp Subst-rate	CY-P1A2 Inhibi-tor	CY-P2C19 Inhibi-tor	CY-P2C9 Inhibi-tor	CY-P2D6 Inhibi-tor	CY-P3A4 Inhibi-tor	Bioa-vaila-bility Score
Docking	Curcumin	3.03	-6.28	High	No	No	No	No	Yes	No	Yes	0.55
	Quercetin	1.23	-7.05	High	No	No	Yes	No	No	Yes	Yes	0.55
	Resveratrol	2.48	-5.47	High	Yes	No	Yes	No	Yes	No	Yes	0.55
	5FU	0.13	-7.73	High	No	No	No	No	No	No	No	0.55
MD	Curcumin	3.05	-6.58	High	No	No	No	No	No	Yes	Yes	0.55
	Quercetin	0.51	-7.48	High	No	No	No	No	No	No	No	0.55
	Resveratrol	2.49	-5.52	High	Yes	No	Yes	No	No	Yes	Yes	0.55
	5FU	0.13	-7.73	High	No	No	No	No	No	No	No	0.55

strong binding with the receptor. This proves that the natural agents curcumin, quercetin, and resveratrol provide much better interactions with the crystal receptor structures of the BRCA1 gene associated with breast cancer (23, 35). In our study, the binding energy results presented in Table 1 indicate that the scores for wild-type and mutant-type BRCA1 receptors are relatively similar. While this finding suggests that the control and experimental group ligands exhibit a broad interaction spectrum, it also raises the possibility of a lack of selectivity between the two receptor types. Reduced selectivity, in particular, could potentially result in off-target effects and lead to drug-related side effects. Nevertheless, this study specifically focuses on evaluating the individual effects of each ligand on BRCA1-related wild-type and mutant-type receptors. It is crucial to highlight that no combinatorial effects of the ligands were investigated within the scope of this study.

Amino acids and interactions formed between mutant type 3FA2 and wild type 3FA2 receptors and other ligands are visualized both after docking and MDS to determine the stability of the complex structures and are shown in Figures 2 and 3. Van der Waals interactions between receptors and ligands, conventional hydrogen bonds, alkyl, and pi-alkyl interactions, amide-pi stacked, unfavorable donor-donor, pi-anion, pi-alkyl, pi-donor interactions, hydrogen bond, and pi-cation interactions can be seen. Conventional hydrogen bonds are observed on these amino acids, facilitating hydrogen bond formation between the curcumin ligand and the hydrogen bond donor (35). Amide-pi interaction type is characterized by the electrostatic attraction forces between the amide hydrogen or carbonyl oxygen of the amide group and the pi-electron cloud in the aromatic ring 34. These interactions occur between aromatic amino acid residues in the active site of the receptor and amide groups in the ligand (35, 36). The resulting interactions and bond types influence the biological activities of the receptor and ligand by enhancing their binding affinity to each other (37). Pi-anion interactions indicate the attractive force between a negatively charged anion group and an aromatic system. Their effect on the receptor and ligand is to assist in identifying specific binding sites (38). Thanks to these interactions, the ligand binds to the receptor more compactly. Unfavorable Donor-Donor Interactions occur when the distance between two hydrogen bond donors is short, but no energy is

sought here (39). This type of interaction can affect the binding energy and stability state of the ligand (39, 40). Pi-donor hydrogen bond and pi-cation interaction types increase the binding affinity by strengthening the stability between the protein and the ligand.

Examining the receptor-ligand complex maps after the molecular docking and molecular dynamics simulation phase is very important in terms of understanding the interactions between structures, the changing behavior of the interactions over time, and the changing behavior depending on the changing environment. Upon inspecting the curcumin complex map in B1 of Figure 3 after MDS, it is observed that amino acids PRO, ALA, Glutamic acid (GLU), and Methionine (MET) are located at positions 610, 613, 655, and 768, respectively. These amino acids and their positions differ from those observed in A1. This variation may be attributed to factors such as receptor and ligand flexibility, solvent effects, and ion interactions. While the docking stage occurs in a simplified solvent or vacuum environment within the in-silico setting, molecular dynamics simulations are typically conducted using solvent models and ions that closely mimic experimental conditions (41). Such environmental distinctions possess the capability to alter the behavior and interactions of the receptor and ligand within the binding region. Despite the presence of different amino acid residues in the wild-type 3FA2 and quercetin complex map in B2, it encompasses the amino acid residues obtained following the docking stage. Nevertheless, certain types of bond interactions between amino acids have undergone alterations. This phenomenon can be attributed to various factors, including binding stability and conformational modifications (37). The consistent identification of the same amino acids obtained during docking through molecular dynamics simulation indicates stable binding between the ligand and the receptor (36). The shift in bond types is indicative of robust interactions. When examining the ligand complex maps of resveratrol in A3 and B3, the sole common amino acid observed is ILE. Generally, all other amino acids exhibit variations. This observation suggests that the binding site of the wild-type 3FA2 receptor displays flexibility, while the ligand undergoes conformational changes. Moreover, they strive to achieve stable binding by minimizing energy when the receptor and ligand interact. The rationale behind this alteration post-docking and MDS is to attain an appropriate docking position that adheres to the specified criteria. The consistent presence of the

ILE amino acid in the receptor-ligand map following both steps signifies its pivotal role in stability during receptor-ligand binding. Overall, upon scrutinizing the receptor-ligand bond maps of the wild-type 3FA2 receptor and various ligands after docking and MDS, it becomes evident that quercetin, with similar amino acid residues and offering the highest stability, stands out. When examining the receptor-ligand maps of the mutant-type 3FA2 and various ligands after docking and MDS in images A1 and B1 in Figure 2, it is observed that the amino acids TRP at position 680, LYS at position 688, SER at position 761, ASP at position 765, and MET at position 768 remain consistent. These findings suggest that the amino acid composition of the mutant-type 3FA2 receptor and the curcumin ligand remains unchanged, indicating stability in the binding interactions and positioning of the complex (41). The fact that the curcumin ligand interacts with the same amino acids in both stages reveals that the conformations of the complex structure are highly minimized (40). The formation of the same receptor-ligand map after docking and MDS shows that the binding affinity is quite good (41). When images A2 and B2 in Figure 3 are examined, it is observed that the amino acids ARG, ASP, and LEU, numbered 705, 763, and 773, respectively, remain unchanged in the quercetin complex map. Additionally, TRP at position 762 and LEU amino acids at position 775 are newly identified following MDS. The persistence of quercetin's interaction with the same amino acids post both docking and MDS suggests the stability of the ligand within the binding site. The emergence of new amino acids after MDS may be attributed to conformational changes in the receptor and ligand-induced by factors such as solvent and ion presence during MDS (38, 41). Furthermore, this phenomenon may be due to the optimization of bonding configurations to minimize energy. When examining the interaction map between the receptor-ligand in A3 and B3, it is observed that only the LYS amino acid number 688 remains consistent with resveratrol after both docking and MDS. With the mutant-type 3FA2 receptor, the resveratrol ligand appears to exhibit significantly lower stability and binding affinity compared to the curcumin and quercetin ligands. In the B4 image in Figure 2, in the complex formed with the 5FU ligand and mutant-type 3FA2, the amino acids GLY at position 681 and SER at position 761 contain carbon-hydrogen bonds, THR at position 682 and GLU at position 740 contain conventional hydrogen bonds, ASP at position 741 contains unfavorable donor-

donor interactions, and HIS at position 685 contains pi-pi stacked interactions. In the B4 image in Figure 3, when examining the interaction of the 5FU ligand and wild-type 3FA2 complex with amino acids, LYS at position 684, GLU at position 740, and SER at position 760 contain conventional hydrogen bonds, and HIS at position 685 contains unfavorable donor-donor and pi-pi stacking interactions.

As a result of the molecular dynamics simulation, RMSF, RDF, RMSD, and Rg analyses were performed. These analyses are conducted to evaluate the stability of receptor-ligand complex structures formed by natural and chemical agents (42). Root Mean Square Fluctuation (RMSF) measures the average deviations in the positions of atoms over time (43). RMSF values serve as analytical tools to evaluate the stability, flexibility, and dynamic behavior of receptor and ligand structures and to understand the conformational changes occurring in the active site of the receptor (42, 43). When the RMSF values of mutant-type and wild-type receptors and ligand complexes in Figure 4 are compared, it is seen that the complexes formed with natural agent ligands are close to the complex formed with chemical drug ligands when the RMSF is examined. This is because natural agents exhibit greater stability with the mutant-type 3FA2 receptor associated with breast cancer and form stronger binding interactions than chemical drugs (12, 42). As a result of RMSF analyses, it is concluded that the structure showing the highest stability among natural agent ligands and mutant-type 3FA2 receptor complexes is the complex formed by the quercetin ligand. This is due to the strong structure and bioactive properties of quercetin (44). From the results of RMSF analyses of wild-type 3FA2 receptors and ligands, it has been revealed that curcumin shows drug potential that can perform various tasks such as regulating the DNA mechanism of the breast cancer-related BRCA1 gene. This shows that curcumin exhibits a strong interaction with the BRCA1 gene receptor associated with breast cancer and has the potential to strengthen the repair mechanism of this gene (45). The fact that both mutant-type and wild-type 3FA2 receptors give the best results with curcumin shows that it has the potential to be an alternative therapeutic agent, especially to the chemical ligand 5FU, in the treatment of breast cancer.

RDF analysis is a mathematical function used to discover the particle pair density of entities such as atoms and molecules located at certain distances

(46). In the field of molecular dynamics simulation, RDF plots are used to analyze distance distributions between proteins and ligands. These RDF plots allow for the investigation of the locations of strong interaction regions between the protein and ligand and the study of the formation mechanisms of complex structures and conformational changes (47). When the RDF graph in Figure 5A is examined, it is seen that the peak values of curcumin and quercetin are more prominent than resveratrol. The sharp peaks in the RDF graphs formed by these two ligands and the mutant-type 3FA2 receptor are interpreted as the ligands providing strong stability and structural order with the receptor structure (42, 46). The absence of distinct peaks in the graph of the resveratrol complex indicates that, according to the RDF definition, atom pairs at a certain distance are distributed over a wide area and the stability of the receptor-ligand complexes decreases (46). As a result of examining the RDF values of the complexes obtained with the mutant-type 3FA2 receptor, it can be said that the curcumin complex is the most suitable. The presence of a single peak in this structure suggests a strong binding affinity between curcumin and the mutant-type 3FA2 receptor. The decrease in RDF values of curcumin beyond a 1 nm distance indicates that there is a specific binding site between the receptor and the ligand. The fact that there is a distinct peak in the RDF graph of the mutant-type 3FA2 complex formed with RDF indicates that it has a specific binding point. In general, good results were obtained in the complexes obtained with the wild-type 3FA2 receptor in Figure 5B. Particularly distinct peaks are observed for quercetin and resveratrol ligands. High RDF values indicate that the interactions between the receptor and the ligand are strong (42, 47). The absence of peaks and lower RDF values in the graphs of curcumin complexes indicate conformational changes in the receptor-ligand binding regions (47). The fact that curcumin does not give the expected RDF results in the wild-type 3FA2 receptor but gives good results in the mutant-type 3FA2 receptor of the BRCA1 gene associated with breast cancer suggests that the natural agent curcumin has the potential to play a therapeutically effective role in BRCA1-induced breast cancer (46, 47). When the values of wild-type 3FA2 and ligands are examined, it appears that the natural agents curcumin, quercetin, and resveratrol have the potential to regulate and repair the BRCA1 gene mechanism (46). However, all three natural agents give similar and good results in mutant-type 3FA2 complexes, such as the complexes

formed with the chemical ligand 5FU, indicating that they are natural therapeutic agents that can be used in cancer treatment.

In mathematical terms, RMSD is the deviation of the mean squares of the positions of atoms over a given time (48). In this study, RMSD plots are used to analyze the stability and structural changes of protein and ligand complexes. The graphs of curcumin and quercetin complexes formed with the mutant-type 3FA2 receptor in Figure 6A show remarkable stability, indicating an extremely compact, stable, and favorable interaction (46). The fact that the values of the resveratrol complex are slightly higher and irregular compared to other natural agent complexes is due to the structure of resveratrol (44). The fact that the RMSD values of the mutant-type 3FA2 receptor and the 5FU chemical ligand are so stable indicates that they have a strong binding affinity. In the RMSD analysis of the complexes formed with wild-type 3FA2 in Figure 6B, it was seen that quercetin, resveratrol, and 5FU formed a more stable graph compared to the other complexes. It shows that the wild-type 3FA2 receptor binds tightly and consistently to the binding site of quercetin and resveratrol ligands (48). The reason why the graph of the receptor-ligand complex formed with the chemical ligand 5FU progresses quite stably is that the chemical structure of the 5FU ligand is quite small and simple, it has a good binding affinity with the receptor, and stable RMSD values are emphasized (29, 46). In our RMSD graphs, it is observed that particularly for wild-type and mutant-type receptors, curcumin and resveratrol ligands show noticeable fluctuations at the beginning of the simulation (44). However, those mentioned ligands are natural agents containing various functional groups and aromatic rings (25). Therefore, they can undergo conformational changes by exhibiting flexibility during binding to the receptor, which can be reflected in the RMSD graphs (48). The fact that each ligand-receptor complex eventually reaches a stable form and that the RMSD values, including fluctuations, remain below 1 nm aligns with values accepted in other literature studies (29). This demonstrates that the protein-ligand complex and the simulation system are stable. Numerous studies by Singh and colleagues suggest that such fluctuations are caused by the dynamic conformational changes of the ligands and the flexibility of the receptor's binding pocket(44). Consequently, the RMSD results obtained in this study fall within the 0 to 1 nm range accepted in the literature and are consistent with

studies indicating that the overall system stability is not adversely affected, as expected.

The term Rg is defined mathematically as the square root of the weighted average of the squares of the distances of their masses, taking the center of mass of the molecules as a reference (49). Within the scope of molecular dynamics simulation, Rg is used to measure the compactness of the protein and ligand complex and to analyze the behavior of the complex over time (50). The reason why there are some fluctuations in the graphs of the complexes obtained with the mutant-type 3FA2 receptor in Figure 7A is that the ligands undergo some conformational changes during binding with the receptor (49). According to the results obtained, it is seen that although the binding stability of resveratrol with the receptor is moderate, it exhibits a strong binding affinity with curcumin. The quercetin ligand also showed positive results within the scope of Rg graphs, revealing that it formed a compact structure with the receptor and the values stabilizing around 2.3 nm after 7.5 ns. Low Rg values and ensuring certain stability are critical features for potential drug candidates in the treatment of BRCA1 gene-related breast cancer (51). When the Rg graphs of the wild-type 3FA2 receptor and different ligand complexes in Figure 7B are examined, the fluctuations in the curcumin complex are much lower than the others, resulting in a more stable and smooth graph. Therefore, it is concluded that the complex formed with curcumin maintains a stable conformation throughout the simulation (50). The quercetin complex with the wild-type 3FA2 receptor appears to stabilize after a certain point. This reveals that there are conformational changes due to increased fluctuations compared to the curcumin results. The observation of greater fluctuation in the 5FU complex and other ligand complexes is due to conformational changes (49, 51). The average Rg values of the 5FU complex were observed to have small fluctuations throughout the simulation, indicating that a stable complex was formed. In conclusion, when the Rg values and graphs are examined, the stability of the graphical fluctuations of the curcumin complex indicates that the complex formed with the wild-type 3FA2 receptor is stable and its binding is compact. This complex has a potentially high affinity. As a result, in wild and mutant-type receptor species, curcumin ligand Rg showed low fluctuations and a stable structure in graphical values and showed the best compactness compared to other complexes (44). Although resveratrol and

quercetin ligands showed good results in terms of Rg value, the fluctuations they showed indicated that both ligands underwent conformational changes. The control group ligand 5FU showed a good stability profile with the receptors, but it did not fully reach the binding properties as good as natural agents (48).

Consisting of five basic concepts: absorption, distribution, metabolism, excretion, and toxicity, ADMET analyzes the pharmacokinetic and pharmacodynamic properties of natural or chemical substances during the drug discovery process (52). While the binding behavior of the ligand to the receptor is examined as a result of docking and MDS, the properties of the ligand in biological systems are examined through ADMET analysis (53). Evaluations from these analyses help to understand the clinical applicability of natural or chemical ligands with discovered therapeutic potential (54). The analyses obtained with SwissADME yield terms such as Consensus Log Po/w value, Log Kp (skin permeability), GI absorption, BBB passage, P-gp substrate, and CYP enzyme inhibitors (53). Considering these concepts, the consensus Log Po/w value represents the lipophilicity level of the ligands (55). A high lipophilicity value of the ligands indicates that they can easily cross the cell membrane. The Log Kp (skin permeability) value indicates the ability of ligands to pass through the skin, and GI absorption indicates the absorption potential in the gastrointestinal tract (52, 55). BBB passage indicates the ability to cross the blood-brain barrier, and P-gp substrate indicates whether the ligand is a substrate for p-glycoprotein (56). CYP enzyme inhibitors show the potential to inhibit P450 (CYP) enzymes (55). ADMET analysis results of ligands after docking and MDS are compared. The reason for this comparative analysis is to measure the stability of data such as the Consensus Log Po/w obtained after the ADMET analysis of the ligands and to determine the stability of the ligands accordingly (54, 56). When the results were examined in general, it was seen that the Log Kp (skin permeability) value obtained after docking in the curcumin ligand decreased after MDS. This can be explained by the fact that during MDS, it is affected by the presence of solvents and ions in the environment, leading to the formation of new interactions (e.g., van der Waals) (54, 57). However, the decrease in this value during MDS indicates an increase in the skin permeability of the ligand. Repeating the ADMET analysis with an in silico experiment is important to ensure the reliability of both the ligand and the resulting data (57, 58).

In both scenarios, the curcumin ligand shows high absorption in the gastrointestinal tract. However, data obtained after docking and MDS lack BBB passage, P-gp substrate, and CYP2C19 and CYP2D6 inhibitors. The lack of BBB passage prevents the curcumin ligand from passing into the central nervous system (53). In this case, if this ligand has any neurotoxic effects, it helps reduce them. However, the lack of BBB permeability of the curcumin ligand intended for breast cancer treatment reveals its inability to reach metastases spread to the central nervous system. The absence of a P-gp substrate indicates the potential to increase the intracellular concentration of the curcumin ligand. Thus, curcumin may exhibit more effective biological activity within the cell. Many drugs are metabolized in the presence of CYP2C19 and CYP2D6 enzymes. The fact that the curcumin ligand does not inhibit these enzymes reduces the risk of side effects that may occur with other drugs. Additionally, the fact that curcumin does not inhibit these enzymes is very important for liver health. When the presence of CYP2C9 and CYP3A4 inhibitors is examined, curcumin shows the potential to remain in the body for a longer time due to this feature. However, these enzymes are also capable of metabolizing many drugs. Therefore, it is important to monitor for possible side effects of curcumin and other medications. The bioavailability score of the curcumin ligand is 0.55, like other ligands, and shows moderate bioavailability and therapeutic properties. This ligand is effectively absorbed into the body orally and is viewed as a potential therapeutic natural agent that specifically targets the breast cancer-associated BRCA1 gene structure (54). When ADMET analyses of other natural ligands were examined, similar data were observed with curcumin. The Log Kp (skin permeability) value of the resveratrol ligand obtained after docking decreased by 5 cm/s after MDS. Although this decrease is relatively small, it indicates that the skin permeability of the resveratrol ligand decreased after simulation (55). In Table 3, the decrease in the Consensus Log P/o (Log Po/w) value of the quercetin ligand after docking and MDS shows that there is a decrease in the lipophilicity of the quercetin ligand, its hydrophobic interactions decrease, and its hydrophilic properties increase. For other ligands, no significant changes were observed in the data obtained after docking and MDS. ADMET analysis results generally show positive results for both mutant-type and wild-type 3FA2 receptors for each natural agent. Based on these analyses, curcumin stands out as the ligand with the most favorable

properties. Subsequent data of docking and post-MDS ADMET assays of the 5FU ligand with mutant-type and wild-type 3FA2 receptors in Tables 2 and 3 are identical. This ligand is generally considered a good medicine. However, low lipophilicity means that it may be inadequate in exceptional cases such as central nervous system metastasis of breast cancer. Therefore, these chemical drug ratios indicate that natural agents have better drug potential (57, 58).

Based on molecular docking and molecular dynamics simulation approaches, this study shows that the natural agents including curcumin, quercetin, and resveratrol may be alternative therapeutic drug candidates to the chemical drug 5FU in the treatment of breast cancer due to the BRCA1 gene mutation. In particular, the fact that curcumin has a good binding interaction score with receptors associated with BRCA1 genes forms a stable structure, and has the expected pharmacokinetic profile is promising for the discovery of new therapeutic natural agents for breast cancer treatment.

Conclusion

Breast cancer arises when normal cells in the breast region undergo abnormal changes, proliferating uncontrollably and forming malignant tumor cells. Gene mutations within the BRCA1 gene, associated with breast cancer, represent significant contributing factors to the advancement of this disease. Various chemical drugs, such as 5FU, are available to prevent harm to this gene and rectify mutations. Nevertheless, chemical drugs often entail numerous side effects that adversely affect the organs of the body, further exacerbating the toll of cancer treatment. Therefore, the discovery of new drug agents of natural origin with minimal side effects presents promising strategies for treating breast cancer associated with BRCA1 gene mutations. In this study, the receptor linked to the BRCA1 gene was identified and point-mutated. Natural agents including curcumin, quercetin, and resveratrol, targeted for discovering anticancer bioactive properties, along with the widely used drug 5FU in the market, were selected for comparison of results. Through separate molecular docking and dynamic simulations with wild-type and mutant-type 3FA2 receptors and other ligands, it was revealed that natural agents offer interactions akin to the chemical drug 5FU. These natural agents demonstrated strong stability with receptors and exhibited favorable pharmacokinetic properties as assessed by ADMET assays. It was observed that curcumin exhibited the

most favorable pharmacokinetic properties among the natural agents, meeting the feasibility criteria for a therapeutic natural drug in the treatment of breast cancer associated with BRCA1 gene mutation. This study underscores the significance of plant-derived natural agents as potential treatments for critical cancer diseases like breast cancer. By shedding light on other literature studies aimed at discovering and developing the bioactive and therapeutic properties of these natural agents, such as their anticancer effects, in the in silico environment, this research offers hope for survival to numerous cancer patients and humanity at large.

Authors' contributions

Conception: DK; Design: NS, DK; Supervision: DK; Data Collection and/or Processing: NS, DK; Analysis-Interpretation: NS, DK; Literature Review: NS; Writing: NS, DK; Critical Review: NS, DK.

References

1.Bozorgi A, Khazaei S, Khademi A, Khazaei M. Natural and herbal compounds targeting breast cancer, a review based on cancer stem cells. Iran J Basic Med Sci. 2020;23(8):970-83.

2.Shiozaki EN, Gu L, Yan N, Shi Y. Structure of the BRCT repeats of BRCA1 bound to a BACH1 phosphopeptide: implications for signaling. Mol Cell. 2004;14(3):405-12.

3.Esteva FJ, Sahin AA, Cristofanilli M, Arun B, Hortobagyi GN. Molecular prognostic factors for breast cancer metastasis and survival. Semin Radiat Oncol. 2002;12(4):319-28.

4.Taghizadeh MS, Niazi A, Moghadam A, Afsharifar A. Experimental, molecular docking and molecular dynamic studies of natural products targeting overexpressed receptors in breast cancer. PLoS One. 2022;17(5):e0267961.

5.Lukasiewicz S, Czeczelewski M, Forma A, Baj J, Sitarz R, Stanislawek A. Breast Cancer-Epidemiology, Risk Factors, Classification, Prognostic Markers, and Current Treatment Strategies-An Updated Review. Cancers (Basel). 2021;13(17).

6.Thirumal Kumar D, Udhaya Kumar S, Jain N, Sowmya B, Balsekar K, Siva R, et al. Computational structural assessment of BReast CAncer type 1 susceptibility protein (BRCA1) and BRCA1-Associated Ring Domain protein 1 (BARD1) mutations on the protein-protein interface. Adv Protein Chem Struct Biol. 2022;130:375-97.

7.Fu X, Tan W, Song Q, Pei H, Li J. BRCA1, and Breast Cancer: Molecular Mechanisms and Therapeutic Strategies. Front Cell Dev Biol. 2022;10:813457.

8.Abu-Helalah M, Azab B, Mubaidin R, Ali D, Jafar H, Alshraideh H, et al. BRCA1 and BRCA2 genes mutations among high-risk breast cancer patients in Jordan. Sci Rep. 2020;10(1):17573.

9.Burguin A, Diorio C, Durocher F. Breast Cancer Treatments: Updates and New Challenges. J Pers Med. 2021;11(8).

10.Sarma H, Kiewhuo K, Jamir E, Sastry GN. In silico investigation on the mutational analysis of BRCA1-BARD1 RING domains and its effect on nucleosome recognition and ubiquitination. Biophys Chem. 2023;300:107070.

11.Bonofiglio D, Giordano C, De Amicis F, Lanzino M, Ando S. Natural Products as Promising Antitumoral Agents in Breast Cancer: Mechanisms of Action and Molecular Targets. Mini Rev Med Chem. 2016;16(8):596-604.

12.Smolarz B, Nowak AZ, Romanowicz H. Breast Cancer-Epidemiology, Classification, Pathogenesis and Treatment (Review of Literature). Cancers (Basel). 2022;14(10).

13.Kopke MM, Aktas B, Ditsch N. Recommendations for the diagnosis and treatment of patients with early breast cancer: update 2023. Curr Opin Obstet Gynecol. 2023;35(1):67-72.

14.Alduais Y, Zhang H, Fan F, Chen J, Chen B. Non-small cell lung cancer (NSCLC): A review of risk factors, diagnosis, and treatment. Medicine (Baltimore). 2023;102(8):e32899.

15.Debien V, De Caluwe A, Wang X, Piccart-Gebhart M, Tuohy VK, Romano E, et al. Immunotherapy in breast cancer: an overview of current strategies and perspectives. NPJ Breast Cancer. 2023;9(1):7.

16.Franzoi MA, Agostinetto E, Perachino M, Del Mastro L, de Azambuja E, Vaz-Luis I, et al. Evidence-based approaches for the management of side-effects of adjuvant endocrine therapy in patients with breast cancer. Lancet Oncol. 2021;22(7):e303-e13.

17.Pawar A, Diwan A, Mahobia V. Complementary and Alternative Medicine Use and Its Impact on the Delayed Presentation and Advanced Stage of Breast Cancer in Newly Diagnosed Indian Women. Indian J Med Paediatr Oncol. 2024;45:495–501.

18.van den Boogaard WMC, Komninos DSJ, Vermeij WP. Chemotherapy Side-Effects: Not All DNA Damage Is Equal. Cancers (Basel). 2022;14(3).

19.Iddrisu M, Aziato L, Dedey F. Psychological and physical effects of breast cancer diagnosis and treatment on young Ghanaian women: a qualitative study. BMC Psychiatry. 2020;20(1):353.

20.Kiewhuo K, Jamir E, Priyadarsinee L, Nagamani S, Sastry GN. Screening of phytochemicals for potential breast cancer targets BRCA1 and BARD1: A network pharmacology approach. Indian J Biochem Bio. 2023;60:393-405.

21.Sarkar E, Khan A, Ahmad R, Misra A, Dua K, Mahdi AA, et al. Synergistic Anticancer Efficacy of Curcumin and Doxorubicin Combination Treatment Inducing S-phase Cell Cycle Arrest in Triple-Negative Breast Cancer Cells: An In Vitro Study. Cureus. 2023;16(12):e75047.

22.Sinha S, Paul S, Acharya SS, Das C, Dash SR, Bhal S, et al. The combination of Resveratrol and PARP inhibitor Olaparib efficiently deregulates the homologous recombination repair

pathway in breast cancer cells through inhibition of TIP60-mediated chromatin relaxation. Med Oncol. 2024;41(2):49.

23.Tran LTT, Dang NYT, Nguyen Le NT, Nguyen HT, Ho DV, Do TT, et al. In Silico and in Vitro Evaluation of Alkaloids from Goniothalamus elegans Ast. for Breast Cancer Treatment. Nat Prod Commun. 2022;17(3).

24.Selvakumar P, Badgeley A, Murphy P, Anwar H, Sharma U, Lawrence K, et al. Flavonoids and Other Polyphenols Act as Epigenetic Modifiers in Breast Cancer. Nutrients. 2020;12(3).

25.Ghobadi N, Asoodeh A. Co-administration of curcumin with other phytochemicals improves anticancer activity by regulating multiple molecular targets. Phytother Res. 2023;37(4):1688-702.

26.Thai TH, Du F, Tsan JT, Jin Y, Phung A, Spillman MA, et al. Mutations in the BRCA1-associated RING domain (BARD1) gene in primary breast, ovarian, and uterine cancers. Hum Mol Genet. 1998;7(2):195-202.

27.Chen T, Yeh HW, Chen PP, Huang WT, Wu CY, Liao TC, et al. BARD1 is an ATPase-activating protein for OLA1. Biochim Biophys Acta Gen Subj. 2022;1866(5):130099.

28.Kruswick A, Lam FC, Kong YW, Smerdon SJ, Yaffe MB. BRCT domains as chromatin readers: Structure, function, and clinical implications. Chrom Read Hea Dis. 2024;35:31-56.

29.Hossain R, Ray P, Sarkar C, Islam MS, Khan RA, Khalipha ABR, et al. Natural Compounds or Their Derivatives against Breast Cancer: A Computational Study. Biomed Res Int. 2022;2022:5886269.

30.Choudhary S, Kesavan AK, Juneja V, Thakur S. Molecular modeling, simulation and docking of Rv1250 protein from Mycobacterium tuberculosis. Front Bioinform. 2023;3:1125479.

31.Dehury B, Raina V, Misra N, Suar M. Effect of mutation on structure, function, and dynamics of receptor binding domain of human SARS-CoV-2 with host cell receptor ACE2: a molecular dynamics simulations study. J Biomol Struct Dyn. 2021;39(18):7231-45.

32.Pettersen EF, Goddard TD, Huang CC, Couch GS, Greenblatt DM, Meng EC, et al. UCSF Chimera--a visualization system for exploratory research and analysis. J Comput Chem. 2004;25(13):1605-12.

33.Zhang Y, Forli S, Omelchenko A, Sanner MF. AutoGridFR: Improvements on AutoDock Affinity Maps and Associated Software Tools. J Comput Chem. 2019;40(32):2882-6.

34.Abraham MJ, Murtola T, Schulz R, Páll S, Smith JC, Hess B, et al. GROMACS: High-performance molecular simulations through multi-level parallelism from laptops to supercomputers. SoftwareX. 2015;1-2:19-25.

35.Chatterjee P, Karn R, Emerson IA, Banerjee S. Docking and Molecular Dynamics Simulation Revealed the Potential Inhibitory Activity of Amygdalin in Triple-Negative Breast Cancer Therapeutics Targeting the BRCT Domain of BARD1 Receptor. Mol Biotechnol. 2024;66(4):718-36.

36.Adasme MF, Linnemann KL, Bolz SN, Kaiser F, Salentin S, Haupt VJ, et al. PLIP 2021: expanding the scope of the protein-ligand interaction profiler to DNA and RNA. Nucleic Acids Res. 2021;49(W1):W530-W4.

37.Bondock S, Albarqi T, Abdou MM, Mohamed NM. Computational insights into novel benzenesulfonamide-1,3,4-thiadiazole hybrids as a possible VEGFR-2 inhibitor: design, synthesis and anticancer evaluation with molecular dynamics studies. New J Chem. 2023;47(44):20602-18.

38.Lin FY, MacKerell AD, Jr. Improved Modeling of Cation-pi and Anion-Ring Interactions Using the Drude Polarizable Empirical Force Field for Proteins. J Comput Chem. 2020;41(5):439-48.

39.Roy A, Anand A, Garg S, Khan MS, Bhasin S, Asghar MN, et al. Structure-Based In Silico Investigation of Agonists for Proteins Involved in Breast Cancer. Evid Based Complement Alternat Med. 2022;2022:7278731.

40.Bilal MS, Ejaz SA, Zargar S, Akhtar N, Wani TA, Riaz N, et al. Computational Investigation of 1, 3, 4 Oxadiazole Derivatives as Lead Inhibitors of VEGFR 2 in Comparison with EGFR: Density Functional Theory, Molecular Docking and Molecular Dynamics Simulation Studies. Biomolecules. 2022;12(11).

41.Ahmad I, Singh AK, Mohd S, Katari SK, Nalamolu RM, Ahmad A, et al. In Silico Insights into the Arsenic Binding Mechanism Deploying Application of Computational Biology-Based Toolsets. ACS Omega. 2024;9(7):7529-44.

42.Skariyachan S, Gopal D, Chakrabarti S, Kempanna P, Uttarkar A, Muddebihalkar AG, et al. Structural and molecular basis of the interaction mechanism of selected drugs towards multiple targets of SARS-CoV-2 by molecular docking and dynamic simulation studies- deciphering the scope of repurposed drugs. Comput Biol Med. 2020;126:104054.

43.Gu S, Shen C, Yu J, Zhao H, Liu H, Liu L, et al. Can molecular dynamics simulations improve predictions of protein-ligand binding affinity with machine learning? Brief Bioinform. 2023;24(2).

44.Munjal NS, Shukla R, Singh TR. Physicochemical characterization of paclitaxel prodrugs with cytochrome 3A4 to correlate solubility and bioavailability implementing molecular docking and simulation studies. J Biomol Struct Dyn. 2022;40(13):5983-95.

45.Muhammad S, Saba A, Khera RA, Al-Sehemi AG, Algarni H, Iqbal J, et al. Virtual screening of potential inhibitor against breast cancer-causing estrogen receptor alpha (ERα): molecular docking and dynamic simulations. Mol Simul. 2022;48(13):1163-74.

46.Hufner-Wulsdorf T, Klebe G. Role of Water Molecules in Protein-Ligand Dissociation and Selectivity Discrimination: Analysis of the Mechanisms and Kinetics of Biomolecular Solvation Using Molecular Dynamics. J Chem Inf Model. 2020;60(3):1818-32.

47.Lamichhane TR, Ghimire MP. Evaluation of SARS-CoV-2

main protease and inhibitor interactions using dihedral angle distributions and radial distribution function. Heliyon. 2021;7(10):e08220.

48.Deshpande SH, Muhsinah AB, Bagewadi ZK, Ankad GM, Mahnashi MH, Yaraguppi DA, et al. In Silico Study on the Interactions, Molecular Docking, Dynamics and Simulation of Potential Compounds from Withania somnifera (L.) Dunal Root against Cancer by Targeting KAT6A. Molecules. 2023;28(3).

49.Rampogu S, Lee G, Park JS, Lee KW, Kim MO. Molecular Docking and Molecular Dynamics Simulations Discover Curcumin Analogue as a Plausible Dual Inhibitor for SARS-CoV-2. Int J Mol Sci. 2022;23(3).

50.Ghahremanian S, Rashidi MM, Raeisi K, Toghraie D. Molecular dynamics simulation approach for discovering potential inhibitors against SARS-CoV-2: A structural review. J Mol Liq. 2022;354:118901.

51.Bhattacharyya J, Bellucci JJ, Weitzhandler I, McDaniel JR, Spasojevic I, Li X, et al. A paclitaxel-loaded recombinant polypeptide nanoparticle outperforms Abraxane in multiple murine cancer models. Nat Commun. 2015;6:7939.

52.El Fadili M, Er-Rajy M, Kara M, Assouguem A, Belhassan A, Alotaibi A, et al. QSAR, ADMET In Silico Pharmacokinetics, Molecular Docking and Molecular Dynamics Studies of Novel Bicyclo (Aryl Methyl) Benzamides as Potent GlyT1 Inhibitors for the Treatment of Schizophrenia. Pharmaceuticals (Basel). 2022;15(6).

53.En-Nahli F, Hajji H, Ouabane M, Aziz Ajana M, Sekatte C, Lakhlifi T, et al. ADMET profiling and molecular docking of pyrazole and pyrazolines derivatives as antimicrobial agents. Arab J Chem. 2023;16(11).

54.Srivastava V, Yadav A, Sarkar P. Molecular docking and ADMET study of bioactive compounds of Glycyrrhiza glabra against main protease of SARS-CoV2. Mater Today Proc. 2022;49:2999-3007.

55.Daina A, Michielin O, Zoete V. SwissADME: a free web tool to evaluate pharmacokinetics, drug-likeness and medicinal chemistry friendliness of small molecules. Sci Rep. 2017;7:42717.

56.Uslu H, Koparir P, Sarac K, Karatepe A. ADME predictions and molecular docking study of some compounds and drugs as potential inhibitors of COVID-19 main protease: A virtual study as comparison of computational results. Med Sci Int Med J. 2021;10(1):18-30.

57.Shah V, Bhaliya J, Patel GM. In silico docking and ADME study of diketene curcumin derivatives (DKC) as an aromatase inhibitor or antagonist to the estrogen-alpha positive receptor (Eralpha(+)): potent application of breast cancer. Struct Chem. 2022;33(2):571-600.

58.Yalcin S. Molecular Docking, Drug Likeness, and ADMET Analyses of Passiflora Compounds as P-Glycoprotein (P-gp) Inhibitor for the Treatment of Cancer. Curr Pharmacol Rep. 2020;6(6):429-40.